# SINGULARITIES OF RADIATION-FLUX ABSORPTION IN A CYLINDRICAL CAVITY

G. E. Gorelik, V. G. Leitsina, and
N. V. Pavlyukevich

UDC 536.3

The distribution of radiation absorbed by the inner surface of a cylindrical cavity is found by the Monte Carlo method for a different nature of the reflection and different ratios between the input beam and cavity diameters.

At this time high-intensity energy sources (laser and electronic) are utilized extensively in heat-treatment processing (hardening, alloying, annealing) of different kinds of metal articles [1, 2]. This method of treatment has a number of advantages: it is local, without deformation, and accurate for parameter regulation, etc. The best results are achieved for normal beam incidence on the surface to be treated. However, for a number of profiled articles it is sufficiently difficult to direct the beam in such a manner even by using specially developed deflectors, and sometimes it is impossible; hence, radiation on the inner surfaces of such articles is mainly incident as a result of multiple reflections.

The energy distribution dependent on the article configuration and the absorption and reflection regularities plays a substantial part in the heat-treatment process.

By using the Monte Carlo method we compute the absorbed energy distribution on the bottom and side surface of a cylindrical cavity of radius R and length L; the origin of coordinates is here at the center of the bottom, while the z axis coincides with the cylinder axis (Fig. 1).

Let us first consider the directional case or radiation that enters the cavity perpendicularly to the bottom, where it is reflected diffusely from the bottom, and both diffusely and specularly from the side surface with a relative magnitude of the specular component $\beta$. The computation is performed for unpolarized radiation in the geometric optics approximation. The method of trial particles is used here, in conformity with which the radiation flux $I_0$ is represented as a set of N identical bunches (trial particles). Each is inserted into the channel with initial coordinates and direction selected in conformity with the radiation intensity distribution in the beam.

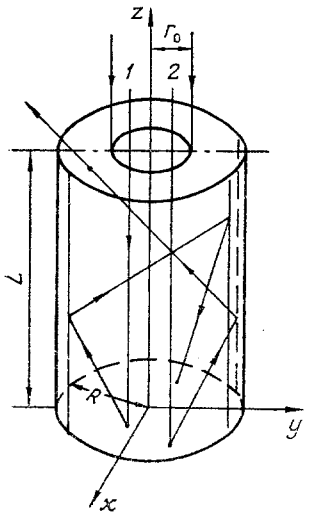


Fig. 1. Diagram of the computation model for a directional source. The trial particle 1 is absorbed on the bottom; the particle 2 emerged from the channel.

A. V. Lykov Institute of Heat and Mass Transfer, Academy of Sciences of the Belorussian SSR, Minsk. Translated from Inzhenerno-Fizicheskii Zhurnal, Vol. 49, No. 2, pp. 304-308, August, 1985. Original article submitted August 16, 1984.

0022-0841/85/4902-0983$09.50  

TABLE 1. Dependence of $2\pi\rho_{max}$ on the Channel Length and the Absorptivity in the Case of a Directional Source with Diffuse Reflection ($r_0$ = 0.5)

| ε | l | | | |
|---|---|---|---|---|
| | 1 | 2 | 5 | 10 |
| 0,1 | 0,12 | 0,16 | 0,19 | 0,21 |
| 0,5 | 0,22 | 0,24 | 0,25 | 0,25 |
| 0,9 | 0,07 | 0,07 | 0,07 | 0,07 |

For a uniform intensity distribution over the beam section, the initial radius of the i-th particle is determined by the following relationship:

$$r_i = [(i - 0{,}5)/N]^{1/2} r_0.$$

The path of the trial particle (the energy bunch) is then tracked until absorbed by the surface or emergence from the channel according to the scheme presented in Fig. 1:

1) The point of trial particle incidence on the bottom or side surface of the channel is determined as the intersection of the rectilinear trajectory

$$\frac{x - x_0}{c_x} = \frac{y - y_0}{c_y} = \frac{z - z_0}{c_z}$$

with the bottom (z = 0) or the cylindrical surface ($x^2 + y^2 = R^2$).

2) An absorption or reflection process is performed according to the given absorptivity ($\varepsilon_b$ on the bottom, $\varepsilon_w$ on the side surface) by using random numbers distributed uniformly between zero and one in the segment.

3) In the absorption case the history of the given trial particle is terminated and consideration of the next particle starts.

4) In the case of reflection, some kind of reflection law is performed according to a given relationship between the diffuse and specular components of the reflected radiation.

5) For a diffusely reflected particle the direction is found from the relation

$$\theta = \arcsin\sqrt{F_\theta}, \quad \varphi = 2\pi F_\varphi,$$

where θ and φ are the polar and azimuthal angles, and $F_\theta$ and $F_\varphi$ the corresponding random numbers.

For specular reflection the direction of the reflected particle $\vec{u}'$ is defined in terms of the direction of the incident particle $\vec{u}$ and the unit normal to the surface $\vec{n}$:

$$\vec{u}' = \vec{u} - 2\vec{n}(\vec{u} \cdot \vec{n}).$$

The process is continued for each particle until it is absorbed or emerges from the channel (Fig. 1).

The quantity of trial particles N selected as a function of the conditions of the problem and of the required accuracy, is 20,000 in this paper.

The program written for an ES type electronic computer in FORTRAN IV permits one to determine the absorbed particles along the cylindrical surface layers and the channel bottom, and also determination of the number of particle emerging from the channel. The absorbed energy distribution over the cavity bottom and side surface as well as the effective absorptivity and the reflection coefficient are thereby found. The mean time for the computation of one version is 3 min.

The dependence of the relative radiation density absorbed by the cylindrical surface on the depth is displayed in Fig. 2 for $\varepsilon_b = \varepsilon_w = \varepsilon$ and $\varepsilon_b \neq \varepsilon_w$ (all the linear dimensions are referred to the channel radius). Results of computations are presented here for a beam filling the whole channel, i.e., with $r_0 = 1$ and a beam with $r_0 = 0.5$. In the first case (dashed curves 1 and 2) the distribution decreases monotonically from a maximum value at

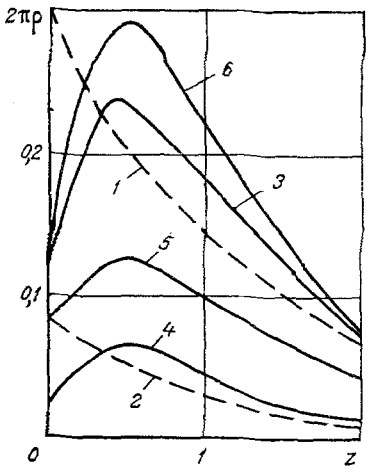


Fig. 2

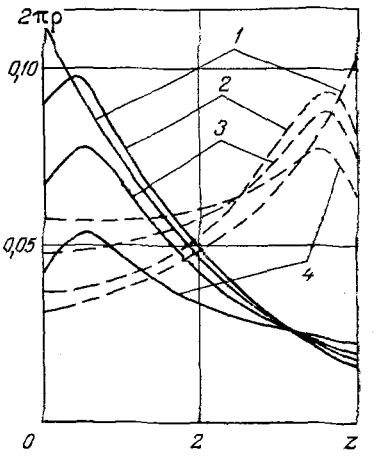


Fig. 3

Fig. 2. Dependence of the absorbed radiation density for a directional source on z for $\tau = 2$; the dashed curves correspond to $r_0 = 1$ (1, $\varepsilon = 0.5$; 2, $\varepsilon = 0.9$); the solid curves to $r_0 = 0.5$ (3, $\varepsilon = 0.5$; 4, $\varepsilon = 0.9$; 5, $\varepsilon_b = 0.5$, $\varepsilon_w = 0.2$; 6, $\varepsilon_b = 0.5$; $\varepsilon_w = 0.8$).

Fig. 3. Dependence of the absorbed radiation density for a directional (solid curves) and diffuse (dashed curves) source for $\tau = 4$, $\varepsilon = 0.2$: 1) $r_0 = 1$, $\beta = 0$; 2) respectively, 0.7 and 0; 3) 0.7 and 0.5; 4) 0.7 and 1.

$z = 0$ (at the bottom), in the second (curves 3 and 4) a maximum is observed at a certain distance $z_{max}$ from the bottom. It is due to the fact that the initial beam is not incident in the annular zone $r_0 < r < 1$ of the bottom, and consequently, the radiation flux directed at the part of the side surface adjoining the bottom diminishes. As $\varepsilon$ grows, the density $\rho_{max}$ (Table 1) and the effective absorptivity $\varkappa_b$ increase and reach maximal values (for $\tau = 2$, $2\pi\rho_{max} = 0.26$ and $\varkappa_{w\,max} = 0{,}33$ for $\varepsilon = 0.45$) and then tend to zero as $\varepsilon \to 1$. Such a nature of the dependence is related to the competition between the absorption processes on the bottom and on the side surface. For a constant $\varepsilon_b$, $\rho_{max}$ grows as $\varepsilon_w$ increases (curves 5, 3, and 6 in Fig. 2).

Computations showed that as the channel length changes the coordinates of the maximum and the dimensions of the characteristic absorption domain change slightly. The quantity $\rho_{max}$ grows slowly here to emerge at a constant value, where the smaller the $\varepsilon$ the more substantial this dependence (Table 1). As the beam radius diminishes, the maximum shifts slowly from the bottom towards the entrance, its absolute value diminishes, and the ratio $\rho_{max}/\rho_0$ characterizing the steepness of the distribution of $\rho$ near the maximum grows.

The absorbed radiation density within the beam limits depends sufficiently weakly on the radius for the bottom, since it drops abruptly (by an order) in the unexposed domain.

TABLE 2. Dependence of the Effective Absorption Characteristics on the Channel Length and the Fraction of the Specular Component for $\varepsilon = 0.2$, $r_0 = 0.7$

| $\tau$ | 2 | | | 10 | | |
|---|---|---|---|---|---|---|
| $\beta$ | 0 | 0,5 | 1 | 0 | 0,5 | 1 |
| | | | Directional Rotation | | | |
| $\varkappa_b$ | 0,260 | 0,229 | 0,197 | 0,278 | 0,245 | 0,202 |
| $\varkappa_w$ | 0,324 | 0,270 | 0,207 | 0,691 | 0,652 | 0,536 |
| | | | Diffuse Rotation | | | |
| $\varkappa_b$ | 0,110 | 0,126 | 0,147 | 0,008 | 0,027 | 0,066 |
| $\varkappa_w$ | 0,438 | 0,444 | 0,424 | 0,646 | 0,749 | 0,852 |

TABLE 3. Comparison of Quantities Characterizing Radiation Absorption in a Channel Computed by the Monte Carlo (MC) Method and from the Solution of the Integral Equation (int) for a Directional Source for $l = 10$, $r_0 = 1$, $\beta = 0$

| $\varepsilon$ | $\varkappa_b$ | | $\varkappa_w$ | | $2\pi\rho_0$ | | $2\pi\rho_1$ | | $2\pi\rho_l$ | |
|---|---|---|---|---|---|---|---|---|---|---|
| | M.C. | int. | M.C. | int. | M.C. | int. | M.C. | int. | M.C. | int. |
| 0,2 | 0,278 | 0,288 | 0,689 | 0,701 | 0,243 | 0,257 | 0,038 | 0,043 | 0,004 | 0,0034 |
| 0,8 | 0,809 | 0,809 | 0,188 | 0,191 | 0,112 | 0,113 | 0,004 | 0,0032 | 0 | $3\cdot10^{-5}$ |

As the fraction of the specular component $\beta$ increases, the density distribution of the absorbed radiation becomes more homogeneous along the cylindrical surface, the maximum shifts towards the entrance, the characteristic dimension of the absorption zone increases (Fig. 3, and the effective coefficients $\varkappa_b$ and $\varkappa_w$ diminish (Table 2).

Let us now consider the case of the diffuse radiation flux incident on the cavity orifice. The absorbed radiation distribution here becomes almost symmetric with respect to a section passing through the middle of the cavity $z = l/2$ (Fig. 3) as compared with an analogous distribution under normal incidence for small $\varepsilon_b$ and large $l$. This is explained by the fact that under normal incidence of radiation the reflection from the bottom is assumed diffuse, while the influence of absorption on the bottom for such $\varepsilon$ and $l$ is not very substantial. Consequently, the integral characteristics for these two cases are similar. Exactly as for normal incidence, if the beam radius is less than the input orifice radius, a maximum is formed in the distribution of $\rho$. As the fraction of the specular component $\beta$ in the reflected radiation grows, the $\rho$ distribution becomes more uniform as before; however, the values of $\varkappa_b$ and $\varkappa_w$ here increase (Table 2), while the maximum shifts towards the bottom (Fig. 3). It should be noted here that the results of computations for diffusely incident radiation for $r_0 = 1$ agree with the data in [3] within the limits of accuracy.

By using the method described it is not difficult to estimate the accuracy of the results obtained in [4] for the case $r_0 = 1$, $\beta = 0$ by solving an integral equation for the radiation-flux density by an approximate analytical method. This method of solution is based on an exponential approximation of the functions in the equation, which characterize the probability of radiation incidence from one element of the channel inner surface on another. It is seen from Table 3 that both methods yield good agreement for both the effective absorptivities $\varkappa_b$ and $\varkappa_w$, and for the relative absorbed radiation densities for different distances from the bottom $z = 0$, $l/2$, $l$ (the densities $\rho_0$, $\rho_1$, $\rho_l$ correspond to these values of z). Let us note that the relative difference in the densities obtained by the above-mentioned methods increases in the domains where they have a minimal value.

Thus, an absorbed radiation density distribution with a maximum at a certain distance from the bottom is formed on the side surface under both normal and diffuse radiation incidence on the diffusely reflecting bottom of a cylindrical cavity for the case $r_0 < 1$ (beam radius less than bottom radius). As the channel length increases, the value of the absorption density at the maximum and the characteristic dimension of the absorption domain vary sufficiently weakly. The absorptivity and the faction of the specular component in the reflected radiation exert considerably more influence on these parameters.

## NOTATION

R, L, cavity radius and length; $r_0$, beam radius; $c_x$, $c_y$, $c_z$, direction cosines of a line; $\varepsilon$, absorptivity; $\rho$, relative density of the absorbed radiation; $\beta$, fraction of the specular component in the reflected radiation; $\varkappa$, effective absorptivity. Subscripts: b, bottom; w, side surface; max, maximum absorbed radiation density.

## LITERATURE CITED


1. L. Satanovskii, "Surface hardening by means of laser and electron beams," Metalloved. Term. Obrab. Met., No. 12, 8-12 (1980).
2. I. B. Borovskii, D. D. Gorodskii, I. M. Sharafeev, and S. F. Moryashchev, "On surface alloying of metals by using continuous laser radiation," Fiz. Khim. Obrab. Mater., No. 1, 19-23 (1984).
3. E. M. Sparrow and R. D. Cess, Radiation Heat Transfer [Russian translation], Énergiya, Leningrad (1971).

4. V. V. Levdansky, V. G. Leitsina, O. G. Martynenko, N. V. Pavlyukevich, and R. I. Soloukhin, "Radiative heat transfer in a model porous body," Proc. VIIth Int. Heat Transfer Conference, Vol. 2, München (1982), pp. 523-527.

# STABLE CONSERVATIVE DIFFERENCE SCHEMES FOR THE QUASILINEAR PARABOLIC HEAT-CONDUCTION EQUATION

V. I. Gladkovskii and V. G. Karolinskii

UDC 518.61:536.242

An efficient algorithm is developed for solving the quasilinear heat-conduction equation using asymmetric difference schemes satisfying the discrete analog of the conservation law.

The optimum regimes of plasma-mechanical treatment (PMT) [1, 2] depend essentially on the temperature field in the surface layer [3]. A more careful examination of processes of interaction of high-intensity heat fluxes with solids leads to the necessity of allowing for the temperature dependence of the thermophysical properties of the material being treated. In order to eliminate structural phase transitions in brittle metals during PMT [4], as well as to prevent the process of development of destructive temperature stresses, it is necessary to provide conditions for the heating of only that part of the volume of the component which is subject to removal [1]. It is proposed to calculate the temperature field in an isolated volume of a half-space by an approximate numerical solution of the quasilinear heat-conduction equation [5], with boundary conditions of the first kind, using explicit, absolutely stable, asymmetric difference schemes (ADS), satisfying a certain discrete analog of the law of conservation of energy, applying averaging by the arithmetic-mean method [6]. The initial ADS are obtained from the heat-conduction equation using the integrointerpolation method [5] with subsequent splitting [7].

It is well known that the numerical solution of problems of mathematical physics imposes especially rigorous demands on both the memory volume and the operating speed of computers [8]. A promising method of overcoming the difficulties arising in the solution of problems of mathematical physics is the use of parallel multiprocessor computer systems [9]. The ADS method has an algorithmic structure not requiring a preliminary procedure of conversion of a sequential algorithm into a parallel one [10] for the programmed execution on multiprocessor computers. The reduction of computer time in the use of multiprocessor computers plays an especially important role in the solution of nonlinear multidimensional problems of mathematical physics.

Let us consider the quasilinear heat-conduction equation

$$\frac{\partial T}{\partial t} = \frac{\partial}{\partial x} k(T) \frac{\partial T}{\partial x}, \tag{1}$$

where $T \geqslant 0$ is the temperature, while the dependence $k(T) \geqslant 0$ of the coefficient of thermal conductivity is assumed to be given. For the unique solvability of the problem it is necessary to assign the boundary conditions

$$T(0, t) = f_1(t), \quad T(l, t) = f_2(t) \tag{2}$$

and initial conditions

$$T(x, 0) = \varphi(x). \tag{3}$$

Introducing the heat-flux function

$$W = k(T) \frac{\partial T}{\partial x}, \tag{4}$$

we rewrite Eq. (1) in the flux form

Brest Engineering-Construction Institute. Translated from Inzhenerno-Fizicheskii Zhurnal, Vol. 49, No. 2, pp. 308-314, August, 1985. Original article submitted July 25, 1984.

0022-0841/85/4902-0987$09.50  